The Resonant Retina: Exploiting Vibration Noise to Optimally Detect Edges in an Image

Max-Olivier Hongler, Yuri López de Meneses, *Member, IEEE*, Antoine Beyeler and Jacques Jacot

Abstract— **We show that, far from being a drawback, the ubiquitous presence of random vibrations in vision systems operating from mobile devices can advantageously be used as fundamental tool for edge detection. Directly inspired by biology, the concept of dynamic retina uses the random spatiotemporal path, traced by a moving receptor that samples the image over time, as the basis for the edge detection operation. We propose a simple mathematical formalization of the dynamic retina concept which shows that the relevant information needed for edge detection is contained in the modulation of the variance of the output signal delivered by the retina. Based on a sequence of observations, we then use a variance estimator to determine the presence of the image edges.**

Following again a biological inspiration, more specifically focusing on neuron dynamics, we introduce a threshold type estimator and use its local asymptotic normality to optimize, via the Cramer-Rao relation, the value of the threshold. The optimal threshold value coincides with a maximum of the associated Fisher information and the overall process can therefore be directly interpreted as a stochastic resonance. We end our contribution by reporting some simple experimental illustrations.

Keywords— **Edge detection, random vibration of the optical axis, microsaccades, threshold variance estimator, Fisher information, Cramer-Rao inequality, stochastic resonance**

I. Introduction

A. Motivation

MANY vision systems set on a mobile platform, such as aerial and satellite cameras, mobile-robotics vision systems and of course biological vision systems, have to deal with noise in the form of random vibrations around their optical axis. This vibration noise is traditionally seen as a nuisance. This paper intends to show that quite to the contrary, this noise can be potentially exploited to extract information that is pertinent enough for edge detection.

Let us consider an individual sensing element, a pixel, of such a vision system, and analyze its output signal along the temporal axis when the sensor is subject to small amplitude vibrations. If the system is viewing a featureless, uniformly lit scene such as in a foggy day, the output is not expected to change much. On the contrary, if the pixel is "seeing" a region of the scene where there is a transition from a dark to light area, such as on the boundary of a dark object against light background, the output signal will constantly vary from low to high levels. Intuitively, higher contrast areas produce an output with higher variability, and the output temporal average is related to the local average intensity. Since high contrast regions are often associated with object boundaries, this approach provides quite a useful information. This observation was first made by Prokopowicz and Cooper [1] and this contribution mathematically formalizes their basic idea and proposes a way to extract the contrast information.

The authors are with the STI/IPR/LPM, Ecole Polytechnique Fédérale de Lausanne, CH-1015 Lausanne, Switzerland. E-mail: max-olivier.hongler@epfl.ch, yuri@ieee.org

B. State of the Art

Ever since vision systems have been mounted on mobile platforms such as planes, satellites [2], cars or more recently mobile robots, engineers have had to tackle the problem of noise in the form of a randon jittering of the optical axis. Until the 90s, the Computer Vision community considered these vibrations of the optical axis as a mere nuisance and developed a wealth of mechanical stabilization systems [2] and filtering techniques [3] to eliminate this ubiquitous jittering.

In parallel to this classical engineering approach, life scientists devoted a strong research activity to the study biological vision systems. One of the interesting contributions of theses studies, was the observation of the presence of small-amplitude movements in the human eye. These excitations are now well known under the name of microsaccades [4][5]. Today the ultimate conclusions concerning the origin, the exact nature and the precise use of these microsaccades are still lacking. Nevertheless, it is clearly established that without these microscopic movements the photoreceptors 'saturate' and the retinal images disappear.

Fully aware of this phenomenon, P. N. Prokopowicz and P. R. Cooper [1] proposed a new vision device, called the *Dynamic Retina* (DR), that *directly takes advantage of the vibrating perturbations generated by mobile robots* or any similar, mobile platforms. The basic idea behind this pioneering work, lies in the fact that the spatiotemporal path, traced by a moving photoreceptor that samples over time, can be used as the basis for neighborhood style image computations, i.e. purely spatial computations. The authors [1] propose a phenomenological description of their DR device and present the results of tests which were performed on an image sequence. There is however no formalization or detailed statistical analysis of the system that would allow its tuning to particular situations. Such a more formal description is one of the aims of the present paper.

The DR concept offers several advantages among others, its massive parallelism and the simplicity of its architecture. Besides applications in the field of mobile robotics [6], the potential interest of the DR concept has been re-

cently further confirmed by several new contributions devoted to biological visual systems. In particular, the studies devoted to the fly [7] and the jumping spider have established the presence of a scanning movement in their compound eyes. These results have further stimulated the conception of several artificial retinas operating in presence of vibrations, [8] [9] [10]. These papers emphasize the resolution-enhancement property that can be achieved by such a scanning movement. This can be achieved if the actual displacement is deterministically known. In particular, periodic motions were discussed in [10].

In the present paper, we offer a generalization which enables to exploit random mechanical excitations of the vision devices. We propose a simple mathematical modeling of the DR device in presence of a noise characterized by its relevant statistical properties. We focus our attention on the edge detection (ED) problem which is of fundamental importance for many vision systems. Indeed, as ED provides a reduction in the amount of visual data, it is the first processing stage common to numerous vision systems ranging from computer vision [11], [12], [13] to biology [14], [15]. Edge detection is particularly difficult in the presence of noise and low light intensity. Our formal approach of the DR in presence of noise clearly exhibits that the relevant part of the information needed to detect the edges of an image is contained in the modulation of the variance of the output random signal. This makes clear that a powerful and reliable inference of the output variance is mandatory and has to be jointly considered.

Taking into account the limited resources of VLSI circuits and also following the "bioinspired" work of [1], we introduce a threshold estimator (TE) typical of spiking-neuron dynamics [16], [17] and [18]. Indeed, the simplest model for neural dynamics considers a single neuron as as a threshold crossing detector in which a cell is stimulated by an external input and if the membrane voltage exceeds a fixed threshold, the cell fires and is reset. Accordingly, for input signals below the threshold value, the neuron does not respond. More precisely, in systems with a threshold, subthreshold signals may generate responses only if noise is added to the original input. In the DR device under study, the random shaking of the optical axis generates the noise which will be added to the input. If the noise is too low, it does not help to cross the threshold value of the detector and nothing is learned from the signal. If, on the other hand, the noise is too high, it will drown the signals and all information will be lost. Intuitively, it is therefore clear that in between, there will be one, (eventually several), optimal noise level(s) for which a maximum of the relevant information regarding the input signal can be inferred. The reliability of such an estimator does therefore intrinsically depend on the suitable choice of the threshold value.

It is expected that the sensory system optimizes this value in order to gather a significant amount of information about the signal. In this paper, we formally implement this optimization algorithm. First, we note that the TE transforms the original DR output process into a binary process (i.e. a Bernoulli process). This process is experimentally characterized by sampling over time the output signal and observe whether the process exceeds or not a given threshold level. This threshold value is then optimized by maximizing the Fisher information that can be associated with the estimation process. This procedure consists in fact in tuning the threshold level in order to have a stochastic resonance [16], [17] and [18] and thus we speak of the *Resonant Retina* (RR) when referring to the DR model together with its optimized TE.

Pioneered two decades ago in science [19], the concept of stochastic resonance (SR) which occurs in the dynamic response of nonlinear systems such as bistable devices [20] and threshold detectors [18], seems to play a growing role in the engineering context [21] and especially in neural dynamics [16]. Roughly speaking, Stochastic Resonance can be viewed as a noise-induced enhancement of the response of a nonlinear system to a weak, external input signal. SR naturally appears in many neural dynamics processes and hence it should not come as a surprise that SR does play a role in vision. So far however, SR has deserved a moderate attention in vision with the notable exception of the dithering process which has recently being revisited from that point of view [22].

The paper is organized as follows: in section II, we formulate the DR concept in a simple mathematical setting. We focus on small noise amplitudes which allow a description in terms of linear response theory and we demonstrate that the relevant contrast information is present in the output signal variance. In section III, we construct a simple estimator (threshold-type estimator (TE)) for the variance and calculate the associated expression for its Fisher information, which affords a direct characterization of the detector performance. The detector shows a stochastic resonance and the optimal threshold is shown to be at the peak of the Fisher information. Section IV, illustrates the DR and TE models for the particular case of Gaussian vibration (colored noise process). In section V, we explicitly work out the general results developed in sections II, III and IV and report experimental results to validate our modeling.

II. Formalization of the Dynamic Retina

In this introductory part, we focus, without loss of generality, on one-dimensional, sampled images. Accordingly, we shall model a grey level image by a function:

$$s : \mathbb{Z} \to K \qquad K = \{0, 1, 2, \ldots, 255\}\,. \tag{1}$$

At the position $x \in \mathbb{Z}$, we say that the image $s(x)$ exhibits a contour when the absolute value of the discrete gradient exceeds a critical value $m > 0$, namely:

$$\begin{aligned} \mid \Delta s(x) \mid \quad &= \quad \mid s(x+1) - s(x) \mid \geq m \\ &\iff \quad \{\exists \text{ a contour at position } x\}\,. \end{aligned} \tag{2}$$

Note that, according to Eq.(1), the discrete derivative fulfills $0 \leq \mid \Delta s(x) \mid \leq k_{\max} = 255$.

Let us now assume that we observe the image $s(x)$ with a camera having its optical axis driven by a noisy signal. This shaking noise of the camera is modeled by a stochastic process $\xi(t)$:

$$\xi : \mathbb{R}^+ \to \Gamma \subset \mathbb{R}. \tag{3}$$

We focus our attention to cases for which the shaking noise process $\xi(t)$ is a stationary stochastic process with vanishing odd stationary moments. According to Eqs.(1) and (3), the input signal in the photoreceptor array is $\eta : \mathbb{Z} \times \mathbb{R}^+ \to K$:

$$\eta(x,t) = s(x + \xi(t)). \tag{4}$$

We define now the temporal low-pass filtered process $\nu(x,t) : \mathbb{Z} \times \mathbb{R}^+ \to \Omega = [0, k_{\max}] \subset \mathbb{R}$ as:

$$\nu(x,t) = \lambda \int_0^t e^{-\lambda(t-s)} \eta(x,s) \mathrm{ds}. \tag{5}$$

Making use of the filtering mechanism described by Eq.(5), the output signal $O(x,t) : \mathbb{Z} \times \mathbb{R}^+ \to [-\Omega, \Omega] \subset \mathbb{R}$ will be given by the highpass filter:

$$O(x,t) = \mathcal{R}\left[\eta(x,t) - \nu(x,t)\right], \tag{6}$$

where $\mathcal{R}$ is a gain factor which will be taken as a positive constant and $\Omega = \mathcal{R} k_{\max}$. Due to the stationarity of $\xi(t)$, the output signal $O(x,t)$ for $t \to \infty$ is itself a stationary stochastic process. Its statistical properties depend on i) the process $\xi(t)$, ii) the filtering process with its cutoff frequency λ in Eq.(5) and iii) the scene function $s(x)$. For future use, let us now introduce the stationary variance $\sigma_o^2(x)$:

$$\sigma_o^2(x) = \langle O^2(x,t) \rangle_s - \langle O(x,t) \rangle_s^2, \tag{7}$$

where $\langle \cdot \rangle_s$ stands for the average operation in the stationary regime. Our goal is to detect the contours of the image function $s(x)$ by using, in an efficient way, the information contained in the output process $O(x,t)$. In particular, the stationary variance given by Eq.(7) does play an essential role. To show this, let us formally rewrite Eq.(4) in the form:

$$\begin{aligned} \eta(x,t) &= \sum_{m=0}^{\infty} s(x)^{(2m+1)} \frac{\xi(t)^{2m+1}}{(2m+1)!} \\ &\quad + \sum_{m=0}^{\infty} s(x)^{(2m)} \frac{\xi(t)^{2m}}{(2m)!}, \end{aligned} \tag{8}$$

where $s(x)^{(k)}$ denotes the k-th discrete derivative of $s(x)$. For small noise amplitudes we can linearize its effect on the signal $\eta(x,t)$ by rewriting Eq.(8) in the form:

$$\begin{aligned} \eta(x,t) &\cong \sum_{m=0}^{\infty} s(x)^{(2m+1)} \frac{\zeta^{2m}}{(2m+1)!} \xi(t) \\ &\quad + \sum_{m=0}^{\infty} s(x)^{(2m)} \frac{\zeta^{2m}}{(2m)!} \end{aligned} \tag{9}$$

where in Eq.(9), we have introduced the stationary moments of the shaking noise, namely:

$$\lim_{t\to\infty} \langle \xi^m(t) \rangle = \begin{cases} \zeta^m & : \quad m \ \text{ even} \\ 0 & : \quad m \ \text{ odd}. \end{cases} \tag{10}$$

Accordingly, we can now rewrite Eq.(9) as:

$$\eta(x,t) \cong A(x) + B(x)\,\xi(t), \tag{11}$$

Proposition 1

The magnitude of the image gradient is present in variance of the output signal $O(x,t)$. Specifically, for any stationary vibration noise that follows Eq.(11), the output signal shows:

$$\begin{aligned} \langle O(x,t) \rangle_s &= 0 \\ \langle O^2(x,t) \rangle_s &\propto B^2(x) \end{aligned} \tag{12}$$

Proof: From Eqs.(5), (10) and (11) it follows that

$$\begin{aligned} \langle O(x,t) \rangle_s &= \langle \eta - \nu \rangle_s = \langle \eta - \eta * h_{lp} \rangle_s \\ &= \langle \eta \rangle_s \cdot (1 - H_{lp}(\omega = 0)) = 0, \end{aligned} \tag{13}$$

where $h_{lp}(t)$ is the filter defined in Eq.(5) and $H_{lp}(\omega) = \frac{\lambda}{j\omega + \lambda}$ is its Fourier transform.

Similarly we have

$$\begin{aligned} \frac{1}{\mathcal{R}} \langle O(x,t)^2 \rangle_s &= \langle (\eta - \nu)^2 \rangle = \langle \eta^2 \rangle - 2\langle \eta\nu \rangle + \langle \nu^2 \rangle \\ &= \langle \eta^2 \rangle - 2R_{\eta\nu}(\tau = 0) + R_{\nu\nu}(\tau = 0) \\ &= A^2(x) + B^2(x)\langle \xi^2 \rangle \\ &\quad - \frac{2}{2\pi} \int_{\infty}^{\infty} S_{\eta\eta}(\omega) H_{lp}(\omega)\, \mathrm{d}\omega \\ &\quad + \frac{1}{2\pi} \int_{-\infty}^{\infty} S_{\eta\eta}(\omega) |H_{lp}(\omega)|^2\, \mathrm{d}\omega, \end{aligned} \tag{14}$$

where $S_{\eta\eta}(\omega)$ stands for the Fourier transform of the autocorrelation function $R_{\eta\eta}(\tau) = \langle \eta(t)\eta(t+\tau) \rangle$. In our case we have:

$$S_{\eta\eta}(\omega) = \mathcal{F}\left\{R_{\eta\eta}(\tau)\right\} = A^2(x) \cdot 2\pi\delta(\omega) + B^2(x) S_{\xi\xi}(\omega), \tag{15}$$

with $\mathcal{F}\{f(t)\} = \int_{-\infty}^{\infty} f(t) e^{-j\omega t}\, \mathrm{d}t$. Plugging Eq.(15) into Eq.(14) we have

$$\langle O^2(x,t)\rangle_s = A^2(x) + B^2(x)\langle \xi^2\rangle_s$$
$$-2\frac{1}{2\pi}\int_{-\infty}^{\infty}\left[A^2 2\pi\delta(\omega) + B^2 S_{\xi\xi}(\omega)\right] H_{lp}(\omega)\,\mathrm{d}\omega$$
$$+\frac{1}{2\pi}\int_{-\infty}^{\infty}\left[A^2 2\pi\delta(\omega) + B^2 S_{\xi\xi}(\omega)\right] |H_{lp}(\omega)|^2\,\mathrm{d}\omega$$
$$= B^2(x)\Big\{\langle \xi^2\rangle_s - 2\frac{1}{2\pi}\int_{-\infty}^{\infty} S_{\xi\xi}(\omega)H_{lp}(\omega)\,\mathrm{d}\omega$$
$$+\frac{1}{2\pi j}\int_{-j\infty}^{j\infty} S_{\xi\xi}(\omega)|H_{lp}(\omega)|^2\,\mathrm{d}s\Big\}, \qquad (16)$$

where once again we use the fact that $H_{lp}(0) = 1$. QED ■

An explicit model with a specific case of $S_{\xi\xi}$ will be presented in section IV. It is now clear that an efficient contour detection will be crucially dependent on the construction of an efficient estimation of the variance $\sigma_o^2(x)$ of the process $O(x,t)$.

III. Threshold estimator of the variance $\sigma_o^2(x)$

There are several different possibilities to estimate the variance of the stochastic process $O(x,t)$. Here, we shall focus on a *threshold estimator* (TE), because it offers the following properties:

i) Adaptability. The threshold D which characterizes the TE can be easily tuned by feedback loops to match drastic changes of the environment [23], such as nonuniform lightning conditions or a dynamic scene.

ii) VLSI compatibility. The TE avoids the squaring present in the Mean Square Deviation (MSD) estimator. Therefore it is easier to implement in resource-limited systems, such as VLSI circuits.

iii) Bioinspiration. The TEs are indeed a basic tool in spiking-neuron dynamics [16] [18] [17] because the simplest model for neural dynamics considers a single neuron as as a threshold crossing detector stimulated by external inputs.

Consider first the binary random variable $\chi(D, \sigma_o^2(x); t)$ defined by:

$$\chi(D, \sigma_o^2(x); t) = \begin{cases} 1 & \mid O(x,t) \mid \geq D \\ 0 & \mid O(x,t) \mid < D, \end{cases} \qquad (17)$$

where $D > 0$ is a threshold parameter that remains to be adjusted in order to get the maximum relevant information needed to estimate $\sigma_o^2(x)$. Note first that for $D \to \infty$, we clearly expect that $\chi(D, \sigma^2(x); t) \equiv 0$ and conversely for $D \to 0$, we will observe $\chi(D, \sigma^2(x); t) \equiv 1$. Clearly, these limiting values of D are not suitable for getting information about $\sigma_o^2(x)$ and hence to detect edges in $s(x)$. In between these two limiting values of D, it will exist one, (or eventually several), optimal value(s) D^* for which the maximum information characterizing $\sigma_o^2(x)$ can be extracted. Let us now formalize this intuitive idea.

Let us first introduce the stationary probability distribution $F_{\sigma_o^2(x)}(u)$ of the output process, namely:

$$\mathrm{Prob}\left\{-\infty \leq O(x,t) \leq u\right\} = F_{\sigma_o^2(x)}(u). \qquad (18)$$

From the ergodicity property of the process $O(x,t)$, we can write:

$$\lim_{N\to\infty}\frac{1}{N}\sum_{k=0}^{N}\chi(D, \sigma_o^2(x); k\Delta t)$$
$$= 2\int_D^{\infty} dF_{\sigma_o^2(x)}(u) =$$
$$= 2\left(1 - F_{\sigma_o^2(x)}(D)\right) = p_{(D,\sigma_o^2(x))} = p(x), \qquad (19)$$

where Δt is a sampling period chosen larger than the typical correlation time of the shaking noise. With this choice of Δt, the random variable $\chi(D, \sigma_o^2(x); k\Delta t)$ are approximately decorrelated. Note that Eq.(19) is in fact an illustration of the Glivenko-Cantelli theorem [24].

From now on, we shall focus on the class of distribution functions $F_{\sigma_o^2(x)}(u)$ that satisfy:

$$F_{\sigma_o^2(x)}(u) = F(\frac{u}{\sigma_o(x)}) \qquad (20)$$

and therefore the probability density function $f(x)$ associated with Eq.(20) satisfies:

$$\frac{d}{du}F(\frac{u}{\sigma_o(x)}) = \frac{1}{\sigma_o(x)}f\left(\frac{u}{\sigma_o(x)}\right). \qquad (21)$$

Note in particular that the Gaussian probability distributions fulfill the properties given by Eqs.(20) and (21).

From Eqs. (19) and (20) we have the relationship:

$$D = \sigma_o(x)F^{-1}(1 - \frac{p(x)}{2}). \qquad (22)$$

We need now to construct an estimator to determine $\sigma_o^2(x)$, via successive observations of the output signal $O(x,t)$.

Let us fix an arbitrary position x and perform a sequence of n observations of the signal $O(x,t)$ at the successive sampling times $k\Delta t$, $k = 1, 2, \ldots n$. Based on these observations, we can define:

$$\hat{p}(x) = \frac{\hat{n}}{n} = \frac{1}{n}\sum_{k=1}^{n}\chi(D, \sigma_o^2(x), k\Delta t), \qquad (23)$$

where $\hat{n}$ is the number of times we have observed $\chi(D, \sigma_o^2(x); k\Delta t) = 1$ for $k = 1, 2, \ldots n$.

For large n, the central limit theorem implies that the standardized error $\sqrt{n}(\hat{p}(x)-p(x))$ will asymptotically approach a Normal random variable with variance $p(x)(1-p(x)) = 4\left[1-F\left(\frac{u}{\sigma^2}\right)\right]\left[F\left(\frac{u}{\sigma^2}\right)-\frac{1}{2}\right]$.
Now we construct the empirical estimator of the variance by writing:

$$\hat{\sigma}_o(x) = \frac{D}{F^{-1}(1-\frac{\hat{p}(x)}{2})}. \tag{24}$$

The meaning of Eq.(24) is now clear. Indeed, knowing the shaking noise distribution $F(x)$ and therefore its inverse and measuring the values of $\hat{p}(x)$, we can infer the variance $\hat{\sigma}_o^2(x)$ of the process $O(x,t)$.

A. Optimization of the threshold parameter D

Proposition 2
With the above definitions, the random variable $\sqrt{n}(\sigma_o - \hat{\sigma_o})$ asymptotically possesses the variance

$$\sigma^2_{\sigma_o} = \frac{\sigma_o^6}{D^2}\frac{\left[1-F\left(\frac{D}{\sigma_o}\right)\right]\left[F\left(\frac{D}{\sigma_o}\right)-\frac{1}{2}\right]}{f^2(\frac{D}{\sigma_o})}. \tag{25}$$

Proof:
For a large number n of experiments, the value $\hat{p}(x)$ will converge with $p(x)$. Let us write:

$$2\epsilon = \hat{p}(x) - p(x)$$

and using Eqs.(22) and (24), we can write:

$$\begin{aligned}
&\sqrt{n}(\sigma_o - \hat{\sigma}_o) = \\
&= \sqrt{n}\left[\frac{D}{F^{-1}(1-\frac{p}{2})} - \frac{D}{F^{-1}(1-\frac{\hat{p}}{2})}\right] \\
&\approx \sqrt{n}\left[\frac{D}{F^{-1}(1-\frac{p}{2})} - \frac{D}{F^{-1}(1-\frac{p}{2})+\epsilon\frac{d}{dy}F^{-1}(y)|_{y=1-\frac{p}{2}}}\right] \\
&\approx \sqrt{n}\left[\frac{D}{F^{-1}(1-\frac{p}{2})} - \frac{D}{F^{-1}(1-\frac{p}{2})}\left[1-\epsilon\frac{\frac{d}{dy}F^{-1}(y)|_{y=1-\frac{p}{2}}}{F^{-1}(1-\frac{p}{2})}\right]\right] \\
&= \sqrt{n}\left[\frac{D}{[F^{-1}(1-\frac{p}{2})]^2}\frac{d}{dy}F^{-1}(y)|_{y=1-\frac{p}{2}}\right]\epsilon.
\end{aligned} \tag{26}$$

Hence, for asymptotically large n, the variance of the estimator in equation (26) is

$$\begin{aligned}
\sigma^2_{\sigma_o} &= \frac{D^2}{[F^{-1}(1-\frac{p}{2})]^4}\left[\frac{d}{dy}F^{-1}(y)|_{y=1-\frac{p}{2}}\right]^2 n<\epsilon^2> \\
&= \frac{D^2}{[F^{-1}(1-\frac{p}{2})]^4}\left[\frac{d}{dy}F^{-1}(y)|_{y=1-\frac{p}{2}}\right]^2 \cdot \\
&\quad \cdot\left(\left[1-F\left(\frac{D}{\sigma_o}\right)\right]\left[F\left(\frac{D}{\sigma_o}\right)-\frac{1}{2}\right]\right).
\end{aligned} \tag{27}$$

Recall that:

$$\begin{aligned}
&\frac{d}{dy}F^{-1}(F(y)) = 1 \rightarrow \\
&\left(\frac{d}{dy}F^{-1}(y)\right)_{|y=F}\cdot\frac{d}{dy}F(y) = 1,
\end{aligned} \tag{28}$$

which, when plugged into equation (27) yields:

$$\begin{aligned}
\sigma^2_{\sigma_o} &= \frac{\sigma_o^2 D^2}{[F^{-1}(1-\frac{p}{2})]^4}\frac{F(\frac{D}{\sigma_o})(1-F(\frac{D}{\sigma_o}))}{f^2(F^{-1}(1-\frac{p}{2}))} \\
&= \frac{\sigma_o^2 D^2}{\frac{D^4}{\sigma_o^4}}\frac{F(\frac{D}{\sigma_o})(1-F(\frac{D}{\sigma_o}))}{f^2(F^{-1}(1-\frac{p}{2}))} \\
&= \frac{\sigma_o^6}{D^2}\frac{\left[1-F\left(\frac{D}{\sigma_o}\right)\right]\left[F\left(\frac{D}{\sigma_o}\right)-\frac{1}{2}\right]}{f^2(\frac{D}{\sigma_o})}.
\end{aligned} \tag{29}$$

QED ■

Following the lines [18], we shall now introduce the concept of Fisher information I_{σ_o} and we use an asymptotic optimality for our estimator together with its local asymptotic normality. Accordingly, the Cramer-Rao bound will be attained in this limit and hence we have:

$$I_{\sigma_o} = \frac{1}{\sigma^2_{\sigma_o}} = \frac{(D^2/\sigma_o^6)f^2(D/\sigma_o)}{\left[1-F\left(\frac{D}{\sigma_o}\right)\right]\left[F\left(\frac{D}{\sigma_o}\right)-\frac{1}{2}\right]}. \tag{30}$$

The optimal estimator at the position x will therefore be determined by the value D_x^* which minimizes the variance $\sigma^2_{\sigma_o}$ of the estimated parameter σ_o. This is precisely the value for which, according to [18], a stochastic resonance arises. Hence the optimal valueD_x^* will be determined by:

$$\frac{\partial}{\partial D} I_{\sigma_o|_{D=D_x^*}} = \frac{\partial}{\partial D} I_{\frac{D}{\sigma_o}|_{D=D_x^*}} = 0. \tag{31}$$

From Eq.(31), it is clear that the optimal threshold D_x^* does explicitly depend on the position x in the image function $s(x)$. In case that the threshold D has to be chosen once for all for the entire image $s(x)$, we adjust it in order to optimally detect the smoothest type of contours, namely those for which the discrete gradient is m.

IV. Explicit illustration for a Gaussian shaking

In this section, we shall perform an explicit analysis for the RR model defined in section II under a particular class of vibration noise, Gaussian noise, of particular relevance in the common vision systems. To this aim, we shall assume that the state space is continuous and $k_{\max} \rightarrow +\infty$. In actual physical systems, the random vibrations will be damped, producing a pink noise. Hence, the camera motion will be represented by an Ornstein-Uhlenbeck process solving the linear stochastic differential equation [25]:

$$d\xi(t) = -\gamma\xi(t)dt + \mu\gamma dW_t, \tag{32}$$

where dW_t is the standard White Gaussian Noise (WGN) process. We shall assume that the process $\xi(t)$ is in its stationary regime and hence the initial conditions needed to solve Eq.(32) will be drawn from a normal (Gaussian) distribution $\mathcal{N}(0, \frac{\mu^2\gamma}{2})$. The shaking process $\xi(t)$ is therefore here modeled by a colored noise with a Lorentzian power spectrum $S_{\xi\xi}(\omega)$, given by:

$$S_{\xi\xi}(\omega) = \frac{\mu^2\gamma^2}{\gamma^2+\omega^2}. \tag{33}$$

Using Eq.(32), we can expand Eq.(4) to get:

$$\begin{aligned}\eta(x,t) &= s(x+\xi(t)) \\ &= s(x)+s'(x)\xi(t) \\ &\quad +\frac{1}{2}s''(x)\xi^2(t)+\frac{1}{6}s'''(x)\xi^3(t)+\dots .\end{aligned} \tag{34}$$

As in section II, we now linearize the noise effect in Eq.(34) which is done by writing:

$$\eta(x,t) = s(x+\xi(t)) \cong$$

$$\cong s(x)+s'(x)\xi(t)+\frac{1}{2}s''(x)\langle\xi(t)\rangle^2 + \frac{1}{6}s'''(x)\langle\xi(t)\rangle^2\xi(t)+\dots . \tag{35}$$

The stationary variance of the process $\xi(t)$ reads as [25]:

$$\langle\xi^2(t)\rangle_s = \frac{\mu^2\gamma}{2}. \tag{36}$$

In view of Eq.(36), we can rewrite Eq.(35) as:

$$\begin{aligned}\eta(x,t) &= s(x+\xi(t)) \cong s(x)+\frac{\mu^2\gamma}{4}s''(x) \\ &\quad +\left[s'(x)+\frac{\mu^2\gamma}{12}s'''(x)\right]\xi(t) = \\ &= A(x)+B(x)\xi(t),\end{aligned} \tag{37}$$

where the definitions are:

$$\begin{aligned}A(x) &= s(x)+\frac{\mu^2\gamma}{4}s''(x) \\ B(x) &= s'(x)+\frac{\mu^2\gamma}{12}s'''(x).\end{aligned} \tag{38}$$

At this stage, we rewrite Eq.(5) in its differential form:

$$\frac{d\nu(x,t)}{dt} = -\lambda\left[\nu(x,t)-\eta(x,t)\right], \tag{39}$$

$$\nu(x,t=0) = 0, \tag{40}$$

and consider now the set of stochastic differential equations defined by Eqs. (32) and (40). The time evolution of $(\xi(t),\nu(x,t))$ constitutes, for a given position x, a degenerate two dimensional diffusion process on $\mathbb{R}\times\mathbb{R}$. The transition probability density $P(u,v,t \mid u_0,v_0,t_0)$ obeys to an associated Fokker-Planck (F-P) equation [25]:

$$\frac{\partial}{\partial t}P(u,v,t \mid u_0,v_0,t_0) = \mathcal{L}P(u,v,t \mid u_0,v_0,t_0), \tag{41}$$

with $P(u,v,t \mid u_0,v_0,t_0)$ being the conditional joint probability density to observe $u \le \xi(t) \le (u+du)$ and $v \le \nu(x,t) \le (v+dv)$. According to Eqs.(32) and (40), the F-P operator reads as:

$$\begin{aligned}\mathcal{L}(\cdot) &= -\frac{\partial}{\partial u}\left[-\gamma u(\cdot)\right]+\frac{\mu^2\gamma^2}{2}\frac{\partial^2}{\partial u^2}(\cdot) \\ &\quad -\frac{\partial}{\partial v}\left[-\lambda(v-A(x)-B(x)u)(\cdot)\right].\end{aligned} \tag{42}$$

In terms of the above definitions, the output signal $O(x,t)$ is written as:

$$O(x,t) = \mathcal{R}\left[A(x)+B(x)\xi(t)-\nu(x,t)\right]. \tag{43}$$

Proposition 3
With the above definition:

$$O(x,t) = \mathcal{R}\hat{O}(x,t), \tag{44}$$

where $\hat{O}(x,t)$ is the stationary stochastic process characterized by:

$$\langle\hat{O}(x,t)\rangle_s = 0 \tag{45}$$

$$\langle\hat{O}^2(x,t)\rangle_s = \frac{\mu^2\gamma^2}{2(\lambda+\gamma)}B^2(x) \tag{46}$$

Proof:
Let us solve the F-P Eq.(41) in the stationary state. This is straightforward as the linearity of Eqs.(32) and (40) implies that the probability measure solving Eq.(41) is a Gaussian. Using Eq.(42) and taking the left hand side of Eq.(41) to be zero, a simple but lengthy algebra yields:

$$\lim_{t\to\infty}P(u,v,t \mid u_0,v_0,t_0) = P_s(u,v) =$$

$$= \mathcal{N}^{-1}\ e^{au^2+2bu(v-A(x))+c(v-A(x))^2}, \tag{47}$$

with the coefficients:

$$a = -\frac{\lambda+\gamma}{\mu^2\gamma^2}, \quad b = \frac{\lambda+\gamma}{\mu^2\gamma^2B(x)},$$

$$c = -\frac{(\lambda+\gamma)^2}{\lambda\mu^2\gamma^2B^2(x)} \tag{48}$$

and $\mathcal{N}$ is the normalization factor.

Using Eq.(48), we obtain:

$$\langle\hat{O}(x,t)\rangle_s = \int_{-\infty}^{\infty}\int_{-\infty}^{\infty}(v-A(x)-B(x)u)P_s(u,v)\,du\,dv = 0 \tag{49}$$

and the variance:

$$\langle \hat{O}^2(x,t)\rangle_s = \int_{-\infty}^{\infty}\int_{-\infty}^{\infty} (v - A(x) - B(x)u)^2 P_s(u,v)\, du\, dv = \frac{\mu^2\gamma^2}{2(\lambda+\gamma)}\, B^2(x). \quad (50)$$

QED ■

Note added in proof. Readers more familiar with signal processing methods will find in appendix A an alternative proof of proposition 3.

From Eqs. (44) and (50), we finally have:

$$\sigma_o^2(x) = \langle O^2(x,t)\rangle_s = \mathcal{R}^2\, \frac{\mu^2\gamma^2}{2(\lambda+\gamma)}\, B^2(x). \quad (51)$$

It is explicit in Eq.(51) that only the odd derivatives of $s(x)$, namely the $B(x)$ terms, modulates the variance of the output process $O(x,t)$. More precisely an ideal contour detection at position x would be achieved if we have:

$$\sigma_o^2(x) \geq \sigma_c^2 \quad \Longrightarrow \quad \exists \text{ a contour at position } x, \quad (52)$$

where in Eq.(52), the critical variance σ_c^2 is obtained by introducing in the factor $B(x)$ given by Eq.(38), the minimal gradient value m, (see Eq.(2) for the condition implying the existence of a contour). Neglecting the contribution due to the third derivative and beyond, we end with:

$$\sigma_c^2 \cong \frac{\mathcal{R}^2\mu^2\gamma^2}{2(\lambda+\gamma)}\, m^2. \quad (53)$$

The Gaussian nature of the process $O(x,t)$, implies that Eq.(20) can be written as:

$$F_{\sigma_o^2(x)}(u) = F(\frac{u}{\sigma_o^2(x)}) = \mathcal{N}\exp\left\{\frac{-u^2}{\mathcal{R}^2\,\frac{\mu^2\gamma^2\,B^2(x)}{2(\lambda+\gamma)}}\right\}. \quad (54)$$

In view of Eq.(30) and (54), the Fisher information reads for this case as:

$$I_{\sigma_0} = \frac{1}{\sigma_o^4}\frac{(\frac{D}{\sigma_o})^2 f^2(D/\sigma_o)}{(F(\frac{D}{\sigma_o})-\frac{1}{2})(1-F(\frac{D}{\sigma_o}))} = \frac{8}{\pi\,\sigma_o^4}\frac{(\frac{D}{\sigma_o})^2\; e^{-(\frac{D}{\sigma_o})^2}}{\left[1-\mathrm{erf}(\frac{(\frac{D}{\sigma_o})}{\sqrt{2}})\right]\mathrm{erf}(\frac{(\frac{D}{\sigma_o})}{\sqrt{2}})}, \quad (55)$$

with the definitions:

$$f(x) =: \frac{1}{\sqrt{2\pi}} e^{-x^2/2},$$

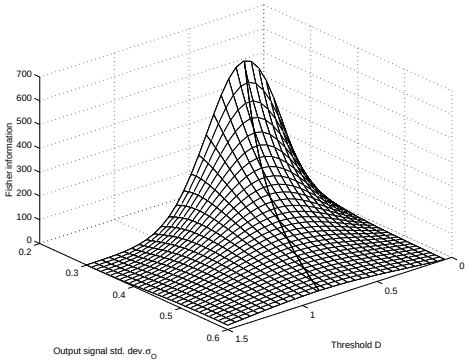

Fig. 1. For a Gaussian vibration the Fisher information, a measure of the estimator quality, shows a resonance peak. The maximum lies on the line given by $D \approx 1.48\sigma_o$.

$$F(z) =: \frac{1}{\sqrt{2\pi}}\int_{-\infty}^{z} e^{-x^2/2}\, \mathrm{d}x = \frac{1}{2} + \frac{1}{2}\mathrm{erf}(\frac{z}{\sqrt{2}})$$

and

$$\mathrm{erf}(z) =: \frac{2}{\sqrt{\pi}}\int_0^z e^{-u^2}\, \mathrm{d}u.$$

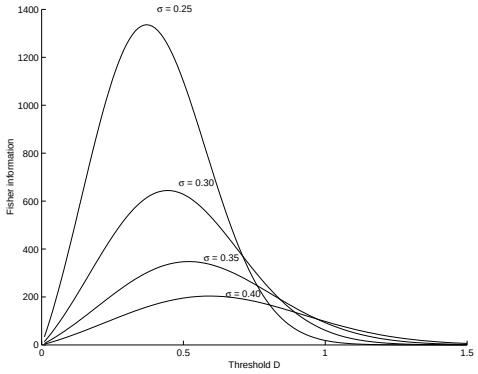

Fig. 2. Fisher information as a function of the threshold D, for 4 different values of σ_o. There is an optimum threshold $D^* \approx 1.48\sigma_o$

The behavior of Eqs.(55) is represented in Figs. 1, 2 and 3 as a function of the threshold D and the output signal standard deviation σ_o, where we clearly see the stochastic resonance effect. The Fisher information given by Eq.(55) shows a peak for the ratio $\frac{D^*}{\sigma_o} = 1.48$. Thus the optimum estimator threshold D^* is linearly dependent on the standard deviation of the output signal of the DR. The DR itself is linearly dependent on the standard deviation of the vibration noise and the magnitude gradient of the scene.

V. Experiments

A. Threshold estimator

The first group of experiments were conducted with the purpose of studying the performance of the Threshold Estimator (TE). Since each pixel works independently from

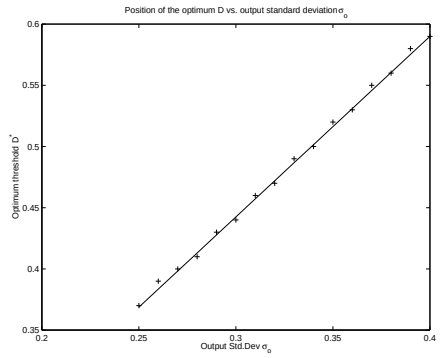

Fig. 3. The optimum threshold D^* depends on the output noise variance with a linear relationship $\frac{D^*}{\sigma_o} \approx 1.48$

its neighbors, a single pixel has been used in a MATLAB simulation. To this end, a white Gaussian noise with standard deviation $\sigma = 2$ was generated and fed to a TE. The noise sample has 100 values. The resulting estimation of the input standard deviation was averaged over 400 trials (realizations) and compared to the Mean Square Deviation (MSD) estimator.

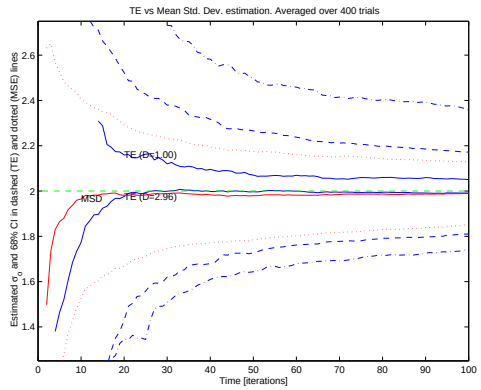

Fig. 4. The threshold estimator (TE) asymptotically converges to actual input standard deviation ($\sigma_{in} = 2$). The results are averaged over 400 trials and 68% confidence intervals are given in dashed and dotted lines.

The results are shown in figure 4, plotting in solid lines the average values estimated by a TE with threshold $D = 2.96$ (the optimum, as shown at the end of section IV) and $D = 1.0$. The dotted and dashed lines correspond to the 68% confidence intervals for TE with $D = 2.96$ (-.-) , $D = 1.0$ (- -) and the MSD estimator ($\cdots$).

The experiments show that the TE is an asymptotically unbiased estimator. Furthermore, the confidence interval is smallest for the MSD estimator, as it is considered the best unbiased estimator for a Gaussian distribution. It can also be seen that the optimum threshold $D = 2.96$ yields a narrower confidence interval compared to the TE with $D = 1$. This shows that the Fisher information is indeed larger for the resonance value $D = 2.96$.

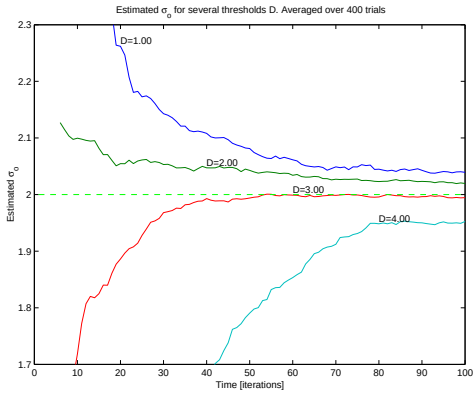

Fig. 5. TEs with different thresholds D. The near-optimum threshold, working on the resonance peak, is $D = 3.00$.

The second experiment compares the estimating capabilities of the TE for different threshold values. The thresholds $D = 1, 2, 3$ and 4 were chosen and the input standard deviation estimated during 100 iterations for an input noise of $\sigma = 2$. The averages of 400 trials are shown in Fig 5. The stochastic resonance effect can clearly be seen, since the estimators with threshold values clearly below ($D = 1$) and above ($D = 4$) the optimum are the slowest to converge, that is, they have the highest variability.

B. Edge detector

After convincing ourselves of the performance of the TE, we proceed on to test the actual Resonant Retina (RR) algorithm. Here we consider not a single pixel but an array of Dynamic Retina pixels with their associated TEs, all with a common threshold D. As before, we have limited ourselves to 1-D images.

Fig. 6. A test image of linearly increasing gradient amplitude.

To this end we use a test image of varying spatial frequency, so that the gradients increase linearly in magnitude from left to right. Fig. 6 shows such an image, and Fig. 7 displays an intensity profile along the x-axis and the corresponding magnitude of its gradient, which can be seen to be linear $|\frac{\partial I}{\partial x}| = kx$ except at discontinuities.

The test image, i.e. the scene in section II, was therefore "shaken" in front of a RR, with a simulated vibration of pink Gaussian distribution, of gain $\mu = 1$ and cutoff frequency (inverse of correlation length) $\gamma = 4$ (cf. Eq. 33). A realization of the input vibration noise $\xi(t)$ and the corresponding output signal $O(256, t)$ is shown in figure 8. The noise amplification is dependent on the local gradient and cutoff frequencies γ and λ, as indicated in Eqs. 51 and 36.

For the first test the RR was tuned with $\lambda = 4$ and 3

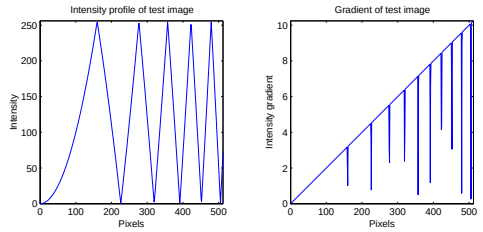

Fig. 7. On the left, the intensity profile of the test image (Fig. 6) along the x-axis. On the right, the magnitude of the gradient along the same axis, showing discontinuities at the peaks and troughs.

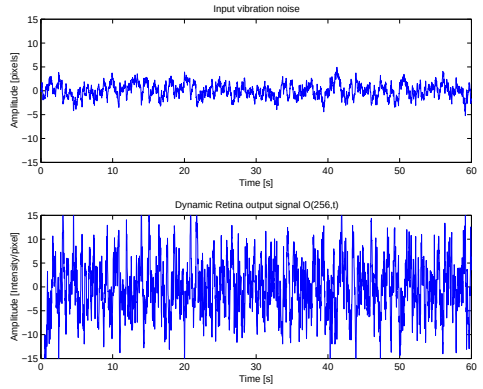

Fig. 8. Input vibration noise and corresponding output signal for pixel $x = 256$. The input vibration noise has a gain $\mu = 1$ and cutoff frequency $\gamma = 4$. The DR has a lowpass filter of $\lambda = 4$.

different thresholds $D = \{1.5, 1.75, 2.0\}$. The stochastic differential equation (32) was integrated during 60 s with steps of 0.02 s using an Euler scheme, which happens to be convergent of order 1.0 for constant coefficients [26]. A single trial was used.

The output of the RR is shown in Fig. 9 and it can be seen that it approximates very well the gradient of the input scene, even at the discontinuities. The actual gradient is shown in dashed linestyle.

Note that the optimal threshold D gives the smallest bias for the estimator when only a limited number of samples are available.

A second test, shown in Fig. 10 shows the results for the same scene, with a noise of slightly lower correlation distance (i.e. higher cutoff frequency of the pink noise), specifically, $\gamma = 8$. As expected from Eq. (51), the output signal standard deviation σ_o increases by a factor $\frac{\gamma}{\sqrt{\gamma+\lambda}} = 1.66$, and therefore so must change the threshold D. Indeed, Fig. 10 shows the results for the same 3 thresholds used in Fig. 9 multiplied by this factor.

A third test was carried out to verify the influence of the noise cutoff frequency γ, the inverse of its correlation length. Figure 11 compares the estimated gradient for three cutoff frequencies $\gamma = \{4, 8, 16\}$, using the same sampling rate $\Delta t = 100$ Hz. If the output signal $O(x, t)$ is

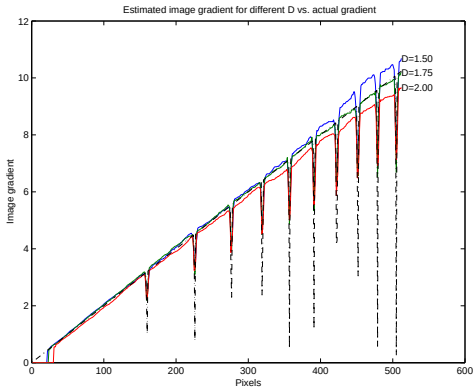

Fig. 9. Estimated gradient image for three different thresholds. The input vibration noise has a variance $\mu = 1$ and cutoff frequency $\gamma = 4$. The DR has a lowpass filter of $\lambda = 4$.

sampled with a period below the correlation distance the samples are correlated an thus an estimator bias appears. As correlation distance is decreased (γ increases) the estimation improves but after a while it becomes faulty once again, as there are more high-frequency contributions than the DR lowpass filter can handle. Moreover, for large γ the noise amplitude becomes too large (cf. Eq. 32) to allow the linearization procedure given by Eq. 35. All three runs were executed with the threshold D set to the optimum for the central pixel, and therefore low gradients to the left of the image is poorly detected.

C. Conclusion

The Resonant Retina (RR), described and analyzed in this paper, is an algorithm for edge detection in a vision system subject to vibration noise. Each pixel of the RR consists of a Dynamic Retina pixel [1] and a parametric variance estimator called Threshold Estimator (TE). A simple mathematical formulation of the dynamic retina subject to random perturbations shows that the information concerning the image gradient (related to the local contrast) is approximately carried by the variance modulation of the output process. Thus, a TE is proposed to extract this gra-

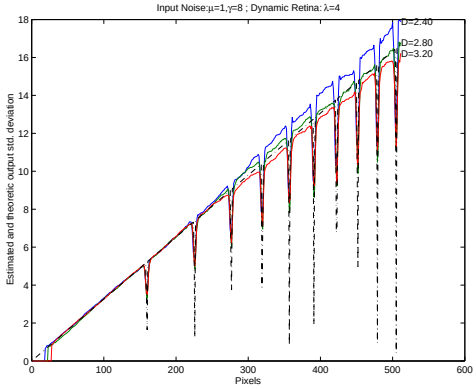

Fig. 10. Estimated gradient image for three different thresholds for a noise of slightly different correlation distance.

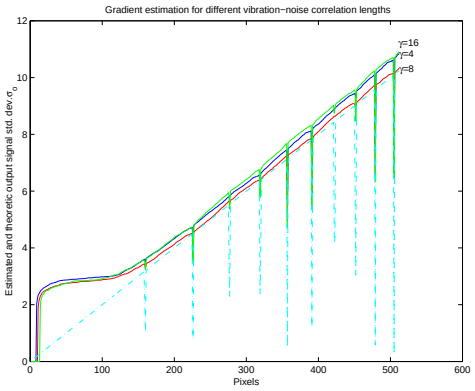

Fig. 11. Estimated gradient image for three different input noise cutoff frequencies γ.

dient information to be used in a subsequent edge detection process. The nonlinear nature of the estimator produces a stochastic resonance that provides an optimization procedure to select the optimal threshold value of the estimator.

In contrast to other works in the field [8] [9] [10] the Resonant Retina works with purely stochastic input. This has practical implications, since it avoids the complicated sensing system required to measure the vibration. In the algorithm described in this contribution, only the first and second order statistics of the perturbation need to be known.

We have purposefully selected an algorithm that allows the system to adapt itself, so that it can be rendered robust against a changing environment –lighting changes, a dynamic scene or a different vibration noise. Three control parameters that can be freely tuned to match a wide range of operating conditions. Namely, our explicit analysis of the role played by the cutoff frequency λ, the output gain $\mathcal{R}$ and the threshold value D, can be used to tune the system. Furthermore, we have shown the existence of an optimum threshold value for a given input vibration noise, and how the Fisher information of the estimator can be used to find this optimum.

A promising contribution of this paper is the use of the Threshold Estimator (TE) to compute the variance of a signal, a tool also used in [18]. Note however that in [18] the TE is used to estimate the average of the signal. In our case, it is the variance that is obtained by such a parametric estimator.

A key feature of the Resonant Retina is that each pixel carries out a relatively simple computation, independently from its neighbors. It is thus particularly advantageous for VLSI implementations, both digital and analog [8]. In the analog world this translates into a massively parallel system –no communication is needed among pixels– of small-size pixels. In the digital one it means less memory requirements, simplified routing (e.g, in FPGA implementations) and, specifically for the TE, that it can be implemented in fixed-point processors.

This massively parallel computation using simple units is reminiscent of biological, neural systems. Although some elements of the Resonant Retina –vibrating noise in form of microsaccades [27] [5], temporal highpass processing on the outer plexiform layer of the retina [15], the Threshold Estimator [16][17]– can be found in biological vision systems, the RR lacks other elements, most notably spatial connections among 'neurons', to be a real model of a biological process. In this paper we rather speak of a "bioinspiration", since we apply some principles taken from biological systems to solve or alleviate an engineering problem.

Finally, it should be clear that despite of the fact that noise contributes to information gathering in the DR system, obviously it does not add any additional information that is not already present in the original, static scene. Noise here merely plays the role of a "catalyst" in the information-gathering process. Yet, the resulting information is pertinent enough for the tasks that follow, namely edge detection and object segmentation.

D. Perspectives

Not considering the ubiquitous presence of noise as a nuisance but on the contrary, trying to use it as a tool in a detection process, is a not-so-common paradigm in the engineering methodology. This contribution inspired by the pioneering work [1], where the idea of a *dynamic retina* is presented, has formally examined the possibility to use the ubiquitous mechanical noise affecting a camera sensing on a mobile platform, to detect the edges of the received images.

This contribution should be considered, from the point of view of actual realizations, as in a preliminary stage. Indeed our experimental approach was restricted to computer simulations. Real environments are likely to generate new difficulties that have not yet been explored. However as long as the noise amplitude remains relatively small, the overall procedure will certainly be robust.

Acknowledgments

We are sincerely grateful to Roger Filliger for numerous suggestions and critiques which enabled us to improve the manuscript.

References

[1] P. Propokopowicz and Cooper, "The Dynamic Retina," *International Journal of Computer Vision*, vol. 16, pp. 191–204, 1995.

[2] Ch. Oliver and S. Quegan, *Understanding Synthetic Aperture Radar Images*, Artech House, London, 1998.

[3] A. Jazwinski, *Stochastic Processes and Filtering Theory*, Academic Press, 1970.

[4] A. Yarbus, *Eye movements and Vision*, Plenum Press, New York, 1967.

[5] J. De Bie, *The control properties of small eye movements*, Ph.D. thesis, Technische Universiteit Delft, 1986.

[6] O. Carmona and Y. Lopez de Meneses, "Etude des mouvements oculaires humains : application à un oeil artificiel," in *Actes des Journées des Jeunes Chercheurs en Robotique (JJCR'8)*, Clermont-Ferrand, France, 1998.

[7] N. Franceschini and R. Chagneux, "Repetitive scanning in the fly compund eye," in *25th Göttingen Neurobiology Conference*, Elsner and Wässle, Eds., 1997, p. 279.

[8] O. Landolt, A. Mitros, and Koch C., "Visual Sensor with Resolution Enhancement by Mechanical Vibrations," in *Proceedings 2001 Conference on Advanced Research in VLSI*, 2001, pp. 249–264.

[9] O. Landolt and A. Mitros, "Visual sensor with resolution enhancement by mechanical vibrations," *Autonomous Robots*, vol. 11, pp. 233–239, 2001.

[10] K. Hoshino, F. Mura, and I. Shimoyama, "A One-Chip Scanning Retina With an Integrated Micromechanical Scanning Actuator," *Journal of Microelectromechanical Systems*, vol. 10, no. 4, pp. 492–497, December 2001.

[11] R. Deriche, "Using Canny's criteria to derive a recursively implemented optimal edge detector," *The International Journal of Computer Vision*, vol. 1, no. 2, pp. 167–187, May 1987.

[12] J. Canny, "A computational approach to edge detection," *IEEE Transactions on Pattern Analysis and Machine Intelligence*, vol. 8, no. 6, pp. 679–697, November 1986.

[13] D. Marr, *Vision*, W.H. Freeman and company, 1982.

[14] D. Hubel, *L'oeil, le cerveau et la vision*, Pour la science. Diffusion Belin, 1994.

[15] W.H.A. Beaudot, *Le traitement neuronal de l'information dans la rétine des vertébrés : Un creuset d'idées pour la vision artificielle*, Ph.D. thesis, INPG, Laboratoire TIRF, Grenoble (France), December 1994.

[16] M. Stemmler, "A single spike suffices: The simplest form of stochastic resonance in model neuron," *Network: Computations in Neural Systems*, vol. 61, no. 7, pp. 687–716, 1996.

[17] U. Müller and L.M. Ward, "Stochastic resonance in a statistical model of a time-integrating detector," *Physical Review E*, vol. 61, no. 4, pp. 4286–4294, April 2000.

[18] P.E. Greenwood, L. M. Ward, and W. Wefelmeyer, "Statistical analysis of stochastic resonance in a simple setting," *Physical Review E*, vol. 60, pp. 4687–4696, 1999.

[19] R. Benzi, A. Sutera, and A. Vulpiani, "The mechanism of stochastic resonance," *Journal of Physics A: Mathematics and General*, vol. 14, pp. L453–L457, 1981.

[20] L. Gammaitoni, Hänggi P., P. Jung, and F. Marchesoni, "Stochastic resonance," *Review of Modern Physics*, vol. 70, no. 1, pp. 223–252, (1998.

[21] B. Ando and S. Graziani, "Adding noise to improve measurement," *IEEE Instrumentation & Measurement Magazine*, vol. 4, no. 1, pp. 24–31, March 2001.

[22] R.A. Wannamaker, S. Lipshitz, and J. Vanderkooy, "Stochastic resonance as dithering," *Physical Review E*, vol. 61, no. 1, pp. 233–236, January 2000.

[23] A. Fairhall, G.D. Lewen, W. Bialek, and R. de Ruyter van Steveninck, "Efficiency and ambiguity in an adaptive neural code," *Nature*, vol. 412, no. 6849, pp. 787–792, Aug 2001.

[24] P. Gänssler and W. Stute, *Wahrscheinlichtkeit Theorie*, Springer Verlag, 1977.

[25] C.W. Gardiner, *Handbook of Stochastic Methods for Physics, Chemistry and the Natural sciences*, Springer Verlag, 1983.

[26] P. Kloeden and E. Platen, *Numerical Solution of Stochastic Differential Equations*, Number 23 in Applications of Mathematics. Springer, 1992.

[27] F. Wörgötter, "Bad design and good performance: Strategies of the visual system fon enhanced scene analysis," in *International Conference on Artificial Neural Networks 2001*. 2001, number 2130 in LNCS, pp. 13–15, Springer.

[28] A. Papoulis, *Probability, Random Variables and Stochastic Processes*, McGraw-Hill, 3rd edition, 1991.

Appendix

I. Alternative proof of Proposition 2

A single pixel of the dynamic retina is described by equations (32), (37), (5) or rather its differential equivalent (40), and (6). The Laplace transform of these equations yields

$$\tilde{\xi}(s) = \frac{\mu\gamma}{s+\gamma}\,\tilde{w}(s) \tag{56}$$

$$\tilde{\eta}(s) = \frac{A}{s} + B\,\tilde{\xi}(s) \tag{57}$$

$$\tilde{\nu}(s) = \frac{\lambda}{s+\lambda}\,\tilde{\eta}(s) \tag{58}$$

$$\tilde{O}(s) = \mathcal{R}\left\{\tilde{\eta}(s) - \tilde{\nu}(s)\right\}. \tag{59}$$

By replacing Eqs. (56), (57) and (58) into Eq. (59) the resulting equation is

$$\tilde{O}(s) = \mathcal{R}\left\{\frac{A}{s+\lambda} + B\frac{s}{s+\lambda}\frac{\mu\gamma}{s+\gamma}\tilde{w}(s)\right\}. \tag{60}$$

The first term disappears in steady-state, and the transfer function of a given pixel is shown to be:

$$\frac{\tilde{O}(s)}{\tilde{w}(s)} = H_{eq}(s) = \mathcal{R}B\mu\gamma\frac{s}{s+\lambda}\frac{1}{s+\gamma}. \tag{61}$$

Each pixel is a linear, time-invariant system driven by a stochastic signal, and thus the statistical properties of the output signal $O(t)$ can be obtained from the statistical properties of the input $w(t)$ and the transfer function of the system $h_{eq}(t)$ [28]. Here we obtain:

$$\langle O(t)\rangle = \langle w(t)\rangle H_{eq}(0) = 0 \tag{62}$$

and

$$\langle O^2(t)\rangle_s = R_{OO}(\tau=0) = \mathcal{F}^{-1}\{S_{OO}(\omega)\}_{|\tau=0} \tag{63}$$

$$= \frac{1}{2\pi}\int_{-\infty}^{\infty} S_{OO}(\omega)\,\mathrm{d}\omega, \tag{64}$$

with

$$S_{OO}(\omega) = S_{ww}(\omega)\cdot H_{eq}(\omega)H_{eq}(-\omega) \tag{65}$$

and $R_{oo}(\tau)$ is the autocorrelation function of $O(t)$. Here we have:

$$\langle O^2(t)\rangle_s = \frac{1}{2\pi}\int_{-\infty}^{\infty}\frac{\mathcal{R}^2B^2\mu^2\gamma^2(\omega^2)}{(\omega^2+\lambda^2)(\omega^2+\gamma^2)}\,\mathrm{d}\omega$$

$$= \frac{\mathcal{R}^2B^2\mu^2\gamma^2}{2\pi}\int_{-j\infty}^{j\infty}\sum_1^4\frac{a_i}{j\omega+p_i}\mathrm{d}\omega, \tag{66}$$

with the poles $p_1 = -p_2 = \lambda$ and $p_3 = -p_4 = \gamma$. The corresponding residues, $a_1 = -a_2 = \frac{-\lambda}{2(\gamma^2-\lambda^2)}$ and $a_3 = -a_4 = \frac{\gamma}{2(\gamma^2-\lambda^2)}$ can be computed and using the Cauchy residues theorem on Eq. (66) we obtain:

$$\langle O^2(t)\rangle_s = \frac{1}{2\pi}\mathcal{R}^2 B^2 \mu^2 \gamma^2 \frac{\pi}{\gamma+\lambda} = \mathcal{R}^2 \frac{\mu^2\gamma^2 B^2}{2(\lambda+\gamma)} \qquad (67)$$

which yields Eq. (51).

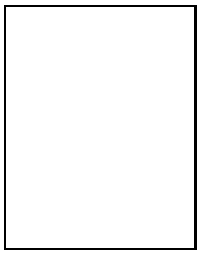

Max-Olivier Hongler received a Doctoral degree in theoretical physics, (in statistical physics), from the University of Geneva, (Switzerland), in 1981. He held several research positions at the Theoretical Physics Dept of the University of Texas at Austin,(U.S.A.), at the University of Toronto, (Canada), the University of Geneva and the University of Lisbon, (Portugal). In 1992-93, he was invited Professor at the Physics department of the University of Bielefeld in Germany. In 1991, he joined the Ecole Polytechnique Fédérale de Lausanne, (Switzerland), where he presently is Professor in the Microengineering department. His present research interests are production flows, stochastic models of manufacturing systems and optimal control in production engineering.

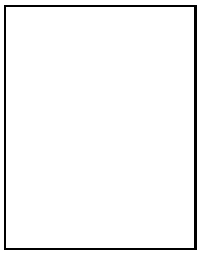

Yuri L. de Meneses received the Engineering degree in Telecommunications from the Polytechnic University of Catalonia, Barcelona, in 1993. He went on to obtain a Masters in Image Processing and Artificial Intelligence at Telecom Bretagne, France (1994) and a MSEE in Control and Robotics from the University of Southern California, Los Angeles (1995). From 1996 to 1999 he completed his Ph.D. at the Ecole Polytechnique Fédérale de Lausanne (EPFL), Switzerland in the field of vision sensors applied to mobile robotics. He is currently Head of the Vision Group at the Institute of Production in Microengineering at the EPFL, where he works in Quality Control, manufacturing process optimization and Computer Vision. His research interests are in Computer Vision for Quality Control, inspection strategy, computational modeling of human visual perception, VLSI vision sensors, manufacturing process optimization and data analysis.

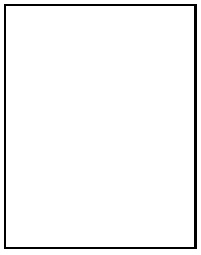

Jacques Jacot obtained an Engineering degree in mechanics from the Ecole Polytechnique Fédérale de Lausanne (EPFL), in 1975, and worked afterwards in the development of assembly robots at the Institut de Microtechnique of the EPFL. From 1976 he has worked in the watchmaking industry. In 1982 he was founder and CTO of Automelec, currently Sysmelec, where he served as CEO from 1989 till 1991. From 1992 till 1994 he was a freelance consultant for the watchmaking industry. In 1994 he was assistant professor in manufacturing techniques at Microengineering Department of the EPFL and promoted to full professorship the next year. In 1998 he becomes the director of the Laboratoire de Production Microtechnique of the aforementioned department. His research interests are in microassembly and packaging of industrial products, optical and vision systems as feedback for assembly and quality control.